Estimation of equilibration time scales from nested fraction approximations

Christian Bartsch,[1,*] Anatoly Dymarsky,[2] Mats H. Lamann,[1] Jiaozi Wang,[1] Robin Steinigeweg,[1] and Jochen Gemmer[1]
[1]*Department of Mathematics/Computer Science/Physics, University of Osnabrück, D-49076 Osnabrück, Germany*
[2]*Department of Physics, University of Kentucky, Lexington, Kentucky 40506, USA*

(Received 13 December 2023; accepted 22 July 2024; published 20 August 2024)

We consider an autocorrelation function of a quantum mechanical system through the lens of the so-called recursive method, by iteratively evaluating Lanczos coefficients or solving a system of coupled differential equations in the Mori formalism. We first show that both methods are mathematically equivalent, each offering certain practical advantages. We then propose an approximation scheme to evaluate the autocorrelation function and use it to estimate the equilibration time τ for the observable in question. With only a handful of Lanczos coefficients as the input, this scheme yields an accurate order of magnitude estimate of τ, matching state-of-the-art numerical approaches. We develop a simple numerical scheme to estimate the precision of our method. We test our approach using several numerical examples exhibiting different relaxation dynamics. Our findings provide a practical way to quantify the equilibration time of isolated quantum systems, a question which is both crucial and notoriously difficult.

DOI: 10.1103/PhysRevE.110.024126

I. INTRODUCTION

How do many-body quantum systems approach equilibrium? The question to quantify this behavior goes back to the advent of quantum mechanics. Considerable progress has been made in the past decades, with concepts like typicality and the eigenstate thermalization hypothesis having been discovered (and sometimes rediscovered) [1]. However, even the question if an expectation value $\langle O(t)\rangle = \mathrm{Tr}\{O(t)\rho\}$ will reach a certain equilibration value after some time T and never depart from it thereafter (until the Poincaré recurrence time, which is usually parametrically much larger than T), for any concrete few-body observable O, Hamiltonian H, and an initial state ρ, cannot currently be answered with certainty. An often used concept in this context is the "equilibration on average" [2]. Here, schematically, the frequency of instants in time at which $\langle O(t)\rangle$ significantly deviates from its temporal average is considered. There are well developed rigorous theorems, asserting this frequency is very small for most practical situations. However, it is very hard (cf. below) to put a bound on the time interval for which this frequency statement applies. Available rigorous bounds are usually too conservative, exceeding physically observed thermalization time by many orders of magnitude. Furthermore, very odd dynamics that are nevertheless in full accord with the principle of equilibration on average have been demonstrated [3]. While it has been shown that, for random Hamiltonians or observables, these equilibration times are typically very short [4–11], it is easy to construct setups for which they are exceedingly long [4,5]. There is an extensive literature establishing bounds on equilibration times, both upper bounds [11,12] as well as lower bounds (often called speed limits) [13]. While these attempts certainly advance the field, many problems limiting their practical applicability remain [14].

In this paper we take a different approach to estimate equilibration time of an isolated quantum system. We focus on the dynamics of autocorrelation functions at infinite temperature, i.e., $C(t) = \mathrm{Tr}\{O(t)O\}$. The latter is in close relation with the dynamics of the expectation values $\langle O(t)\rangle$ for a great variety of initial out of equilibrium states ρ [15,16]. The time dynamics of $C(t)$ can be expressed using the recursion method or in the Mori formalism. Both approaches parametrize $C(t)$ in terms of a sequence of positive numbers b_n, called the Lanczos coefficients, which are defined by the pair O, H. One observes that these numbers are the same in both pictures. We propose an approximation scheme and define $C^R(t)$, an approximation to $C(t)$, defined in terms of the first R Lanczos coefficients. Technically, $C^R(t)$ is defined by leaving first R coefficients b_n intact and declaring $b_n = b_R$ for $n \geqslant R$. Strictly speaking $C^R(t)$ coincides with $C(t)$ only in the limit $R \to \infty$, but importantly it gives a reasonable approximation for a wide range of times already for moderate values of R. To select an appropriate number R we develop a criterion based on a pertinent area measure for the area under the curve $C^R(t)$, which constitutes an essential part of our approach. We then use $C^R(t)$ to estimate the thermalization time for a number of standard observables and Hamiltonians and find that our method yields reasonable accuracy across the board already with $R < 10$. Since computing the first 10 or so Lanczos coefficients for local observables and Hamiltonians with local interactions is usually a straightforward and simple numerical task, our approach readily provides a practical way to estimate the equilibration time for many quantum systems and observables. To summarize, our estimate is not a rigorous bound, but turns out to be very reasonable in all considered examples. Related approaches can be found in [1] and [5], but for in a sense specific types of Hamiltonians and observables, and in

*Contact author: cbartsch@uos.de

[11] and [12]. Shortcomings of the approach in [11] and [12] are pointed out in [14].

This manuscript is organized as follows. First, we present a scheme to obtain an approximation for the autocorrelation function within the Mori picture, define suitable equilibration times, and establish a convergence criterion based on a pertinent area measure in Sec. II. Finally, we numerically test our approach for different types of quantum dynamics in Sec. III. Brief overviews about the Lanczos and the Mori approach to autocorrelation functions are provided in Appendixes A and B, respectively.

II. APPROXIMATION OF DYNAMICS

The object of interest is the infinite temperature autocorrelation function of the form

$$C_0(t) = \mathrm{Tr}\{O(t)O\} \tag{1}$$

with some pertinent observable O. Here, $O(t)$ denotes the time dependence in the Heisenberg picture, $O(t) = e^{iHt}\, O\, e^{-iHt}$, induced by the corresponding Hamiltonian H ($\hbar$ set to 1). O is assumed to be normalized according to $\mathrm{Tr}\{O^\dagger O\} = 1$. The dynamics of $C_0(t)$ can be accessed via the recursive method (Appendix A) or the Mori approach (Appendix B). In both cases the autocorrelation function is determined by the Lanczos coefficients b_n. For a local operator O and a Hamiltonian with local interactions, the first coefficients b_n, up to n of the order of the system size, are system size independent, in particular b_1. This is an important observation allowing us later to estimate the thermalization time of $C(t)$ in the thermalization limit, when the system is taken to infinity.

A. Memory-kernel approximation

Our main proposal is that the exact dynamics for $C_0(t)$ may be reasonably approximated by a suitably "truncated" continuous fraction, not in the sense that the resulting approximate correlation function is very close to $C_0(t)$ for all t, but that it has approximately the same early t behavior and hence equilibration time (defined below).

Our "truncation" scheme does not assume rendering the sequence of b_n finite, but rather we propose to leave the first R coefficients b_n intact, while setting all subsequent Lanczos coefficients to be constant $b_n = b_R$ for all $n \geqslant R$. Although this may seem to be a radical step from the Lanczos algorithm point of view, it yields a good approximation, as we see below.

From the Mori viewpoint, rendering all $\Delta_n = b_R$ constant for $n \geqslant R$ results in a successive application of the same map:

$$\tilde{C}_{n-1}(\omega) = \frac{1}{i\omega + b_R^2 \tilde{C}_n(\omega)}. \tag{2}$$

Here, instead of s we used $s = a + i\omega$ and note that knowing $\tilde{C}_n(s)$ along the imaginary axis is sufficient to perform the inverse Fourier transform and determine $C_n(t)$. Successive application of the same transform makes all $\tilde{C}_n(\omega)$ for $n \geqslant R-1$ the same and equal to a fixed point of the map $\tilde{C}_n(\omega) = \tilde{S}_R(\omega)$ for $n \geqslant R-1$, where

$$\tilde{S}_R(\omega) = -i\frac{\omega}{2b_R^2} + \frac{1}{b_R}\sqrt{1 - \left(\frac{\omega}{2b_R}\right)^2} \tag{3}$$

for $|\omega| \leqslant 2b_R$ and

$$\tilde{S}_R(\omega) = i\left(-\frac{\omega}{2b_R^2} + \mathrm{sgn}(\omega)\frac{1}{b_R}\sqrt{\left(\frac{\omega}{2b_R}\right)^2 - 1}\right) \tag{4}$$

otherwise. Here $\mathrm{sgn}(\omega)$ is the sign function. This result already first appears in [17].

As a result we get the following approximation $\tilde{C}_R(\omega)$ to the original exact $\tilde{C}_0(\omega)$: with all kernels $\tilde{C}_n(\omega)$ being equal to each other for $n \geqslant R-1$ the continued fraction expansion becomes finite, e.g., for $R = 3$,

$$\tilde{C}_0^{R=3}(\omega) = \cfrac{1}{i\omega + \cfrac{b_1^2}{i\omega + \cfrac{b_2^2}{i\omega + b_3^2 \tilde{S}_3(\omega)}}}. \tag{5}$$

Overall, this approximation is expected to be more accurate as R increases. However, our main point is that in many practical situations it yields a reasonably accurate approximation already for small R ($\leqslant 10$). In such a case, the Fourier transform of $\tilde{C}_0^R(\omega)$ can be readily evaluated numerically, giving rise to $C^R(t)$. The resulting approximation is therefore determined by a very small number of Lanczos coefficients, b_n with $n \leqslant R$, but, as we see below, gives a good approximation to $C_0(t)$ for a wide range of t.

B. Equilibration time

We define the equilibration time τ as the time when the absolute value of $C(t)$ drops below some threshold value g and never exceeds it again, i.e., $|C(t)| \leqslant g$ for $t \geqslant \tau$, for which we can calculate $C(t)$ numerically. This excludes, in particular, the Poincaré recurrence. Similarly, we denote the equilibration time of C^R by τ_a (approximate equilibration time) and $|C^R(t)| \leqslant g$ for $t \geqslant \tau_a$. Our definition differs from other definitions of equilibration time in the literate, e.g., Ref. [12]. It is best suited for situations when $C(t)$ decays sufficiently fast. Physically, τ is characterizing local equilibration. Indeed in most cases τ is finite in the thermodynamic limit, while global thermalization time, i.e., diffusion time associated with $C(t) \sim t^{-1/2}$ in 1D systems, would increase indefinitely with the system size.

Put differently, the definition above is not sensitive to functional behavior of $C(t)$ for large t; see the discussion in [18,19]. Thus even if there is a slow decaying long tail, e.g., $\propto 1/t^\alpha$, $\alpha > 0$, which is known to be sensitive to b_n with very large n, the equilibration time τ may still be sensitive only to a handful of first b_n.

Our approach is to estimate τ by evaluating τ_a. To characterize the resulting discrepancy we introduce a relative error defined as

$$\varepsilon_{\tau,R} = \left|\frac{\tau_a - \tau}{\min(\tau_a, \tau)}\right|. \tag{6}$$

C. Area estimate and equilibration time

Since the evaluation of $\varepsilon_{\tau,R}$ is not possible without knowledge of the exact τ, below we propose an indirect method to control the precision. Namely, we introduce another measure of precision to determine the minimal suitable value of R.

To assess the precision, we introduce the "area measure" defined as the area under $C^R(t)$,

$$A_R = \int_0^\infty C^R(t)dt = \tilde{C}_0^R(0). \tag{7}$$

This measure is easy to calculate analytically, yielding

$$A_R = \frac{1}{b_1}\Pi_{n=1}^{R-1}\left(\frac{b_n}{b_{n+1}}\right)^{(-1)^n}. \tag{8}$$

In a similar way we introduce the area under the exact $C(t)$, $A = \tilde{C}_0(0)$.

The approximated correlation function $C^R(t)$ can only be a good description of $C(t)$ so far as the area measures for both are not significantly different from each other. When R increases, A_R will converge to A (this statement is intuitive but mathematically subtle; see [20]). We intend to choose R as small as possible, so that A_R will not be too different from A. As a measure of convergence we can use the relative error

$$\varepsilon_{A,R} = \frac{1}{2}\left(\frac{|A_R - A_{R+1}|}{A_R} + \frac{|A_R - A_{R+2}|}{A_R}\right) \tag{9}$$

and choose the smallest R, for which $\varepsilon_{A,R}$ falls below some predefined threshold a.

We emphasize that evaluating the area measure (8) is easy and only requires a small number of Lanczos coefficients.

As a consistency check of our proposal we note that, for typical quantum systems satisfying the universal operator growth hypothesis of [18] and exhibiting linear growth of Lanczos coefficients $b_n = c\,n + d$, the area measure A_R converges with the rate $1/R$. We consider an example of a system exhibiting such a behavior below.

There are certainly examples where the area A and hence the approximation (8) diverges, e.g., autocorrelation functions of on-site spin operators in a diffusive 1D spin system, which decays as $\propto 1/\sqrt{t}$. In this case our area-based indirect measure of accuracy is not applicable, although the approach of estimating τ using $C^R(t)$ may still hold.

In the following, our goal is to demonstrate that there is a correlation between the relative area error $\varepsilon_{A,R}$ and the relative equilibration-time error $\varepsilon_{\tau,R}$ such that if $\varepsilon_{A,R}$ is reasonably small, then $\varepsilon_{\tau,R}$ is relatively small as well, which in turn means that τ_a is a reasonable approximation for τ. We show this numerically for several models with different archetypal dynamics.

D. Example: SYK model

First, to illustrate the approach above we consider a standard example of a quantum chaotic system—the Sachdev-Ye-Kitaev (SYK) model describing N interacting Majorana fermions [21]. This case can be treated semianalytically, i.e., in a certain limit Lanczos coefficients and correlation functions can be obtained analytically. In the large q limit, where q is the number of fermions in the interacting term, the correlation function and the Lanczos coefficients can be described analytically,

$$C(t) = \frac{1}{\cosh^\eta(\alpha t)}, \quad b_n^2 = \alpha^2 n(n+\eta-1), \tag{10}$$

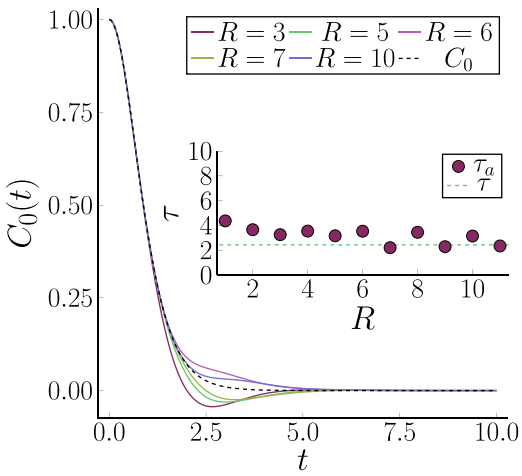

FIG. 1. Actual and approximated correlation functions for different values of R for the SYK model with $\eta = 2$. Inset shows equilibration times of approximated correlation functions for different values of R with equilibration-time threshold $g = 0.03$.

with some positive α, η. The same $C(t)$ and b_n appear in the context of 2D conformal field theories, with α being related to inverse temperature and η to the operator's dimension [22]. The correlation function (10) is decaying exponentially, with the "area measure" (7)

$$A = \frac{\Gamma(1/2)\Gamma(\eta/2)}{2\alpha\Gamma[(1+\eta)/2]} \tag{11}$$

and thermalization time $\tau \approx -\ln g/(\alpha\eta)$.

Now we use our approximation scheme by changing all b_n for $n \geqslant R$ to be $b_n = b_R$. This behavior is very accurately describing actual Lanczos coefficients in a model of a 1D free scalar field, with a UV cutoff of order b_R; see [23]. As one may expect, a UV cutoff does not significantly affect the two-point function until the times inversely proportional to its value. Accordingly, the area measure of the new correlation function (8), which can be evaluated analytically, converges to the true result with the $1/R$ rate,

$$\begin{aligned} A_R &= \frac{\sqrt{\pi}\,\Gamma\left(\frac{\eta}{2}\right)\sqrt{\frac{\eta+R-1}{R}}\,\Gamma\left(\frac{R+1}{2}\right)\Gamma\left(\frac{R+\eta}{2}\right)}{2\Gamma\left(\frac{\eta+1}{2}\right)\Gamma\left(\frac{R}{2}\right)\Gamma\left(\frac{1}{2}(R+\eta+1)\right)} \\ &= A\left(1 - \frac{1}{2R} + \frac{2\eta-1}{8R^2} + \cdots\right). \end{aligned} \tag{12}$$

This confirms that taking $R \approx 10$ would provide a reasonably good accuracy for the estimation of the area measure. Similarly, τ_a will give a reasonable approximation to τ, as follows from the numerical plot of $C^R(t)$ in Fig. 1.

III. NUMERICS

In the following, we test our approach numerically for several typical quantum models. Generally these models are all relevant in the context of condensed matter physics and are chosen to cover a wide range of different types of dynamics as well as a wide range of equilibration time scales.

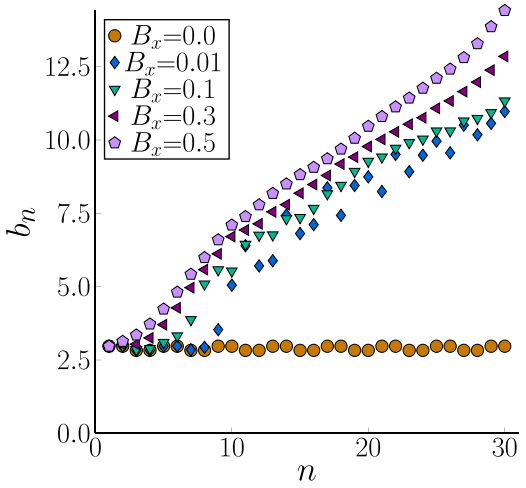

FIG. 2. Numerically calculated Lanczos coefficients for the tilted-field Ising model.

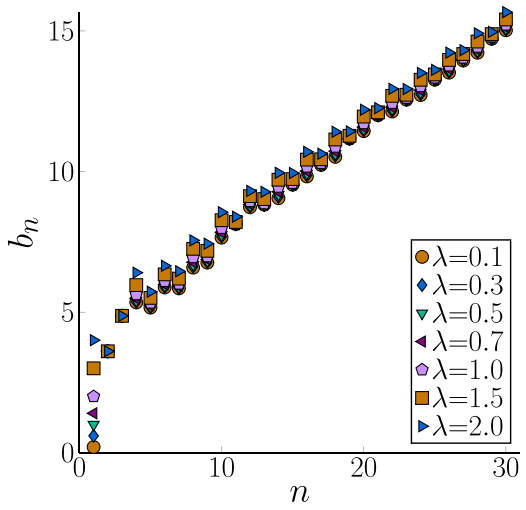

FIG. 3. Numerically calculated Lanczos coefficients for σ_z^S in the model of a spin-1/2 coupled to a bath.

A. Tilted-field Ising model

We begin with the tilted-field Ising model, i.e., an Ising spin chain with a tilted magnetic field that has components along two directions (here x and z). This model is an example for the type of models consisting of a system without a bath. The Hamiltonian reads

$$H = H_0 + B_x \sum_l \sigma_x^l, \tag{13}$$

$$H_0 = \sum_l J\sigma_x^l \sigma_x^{l+1} + B_z \sigma_z^l, \tag{14}$$

where $\sigma_{x,z}$ are the respective spin components, J is the spin coupling constant, and $B_{x,z}$ are the components of the applied magnetic field. We set $J = 1.0$, $B_z = -1.05$ and use B_x as a tunable parameter. For $B_x = 0$ the magnetic field is not tilted and the model is integrable, whereas for $B_x \neq 0$ the model becomes nonintegrable. As an observable of interest, we consider a fast mode [24]

$$O \propto \sum_l \cos(\pi l) h_l, \tag{15}$$

with h_l being the local energy, i.e., $H = \sum_l h_l$,

$$h_l = J\sigma_l^x \sigma_{l+1}^x + \frac{B_x}{2}\left(\sigma_l^x + \sigma_{l+1}^x\right) + \frac{B_z}{2}\left(\sigma_l^z + \sigma_{l+1}^z\right). \tag{16}$$

For the calculation, we choose a system with $L = 24$ spins and periodic boundary conditions. The dynamics of this observable is the case of a rather fast decaying correlation function; for a further discussion see [25]; the corresponding equilibration time is rather short. The finite length L is only relevant for the numerical calculation of the actual correlation function.

Corresponding Lanczos coefficients are depicted in Fig. 2. These coefficients are system size independent. Their values are obtained by increasing the length L to be large enough such that finite size effects vanish. (For this model the first $L/2$ Lanczos coefficients correspond to infinite-system values.)

B. Spin-1/2 coupled to an Ising spin bath

Next, we consider a model of a single spin-1/2 coupled to a bath, which consists of an Ising spin model with an applied magnetic field. This model is an example for the type of models consisting of a system and a bath. The corresponding Hamiltonian reads

$$H = H_S + \lambda H_I + H_B, \tag{17}$$

with

$$H_S = \omega \sigma_z^S, \tag{18}$$

$$H_I = \sigma_x^S \sigma_x^0, \tag{19}$$

$$H_B = \sum_l J\sigma_z^l \sigma_z^{l+1} + B_x \sigma_x^l + B_z \sigma_z^l. \tag{20}$$

The parameters are chosen to be

$$\omega = 1, \quad J = 1, \quad B_x = 1, \quad B_z = 0.5. \tag{21}$$

The length of the bath is $L = 20$ and we use periodic boundary conditions. Finite L effects are only important for the exact $C(t)$; all evaluated b_n are universal. Here H_S is the Hamiltonian of the single spin, H_B is the bath Hamiltonian, and H_I introduces a coupling of the single spin to the first spin of the bath via the corresponding x components. We investigate different scenarios for this model by varying the coupling strength λ. As observables of interest for the correlation function, we analyze here the z component of the single spin, $O = \sigma_z^S$, and the respective x component, $O = \sigma_x^S$.

The Lanczos coefficients are shown in Figs. 3 and 4. Note that for both observables all Lanczos coefficients, except for the first one, are very similar. For the observable σ_z^S, the first Lanczos coefficient b_1 is much smaller compared to the others b_n's. It decreases for smaller interaction strength λ. For the observable σ_x^S, similar behavior is exhibited by the second Lanczos coefficient b_2. This feature has an immediate consequence for the value of A_R. For small coupling strengths λ, the observable σ_z^S exhibits a slow exponential decay and σ_x^S exhibits a slow, exponentially damped oscillation [26]; see

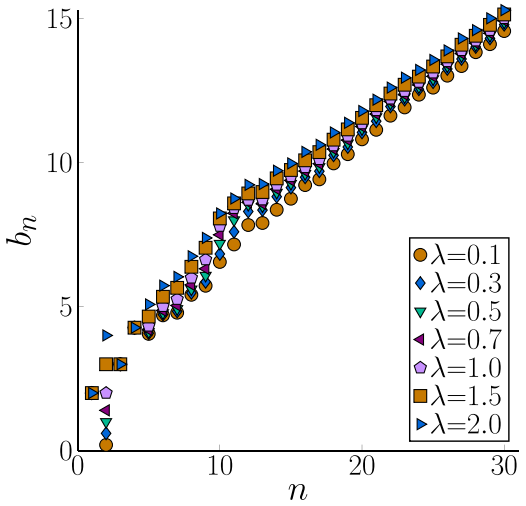

FIG. 4. Numerically calculated Lanczos coefficients for σ_x^S in the model of a spin-1/2 coupled to a bath.

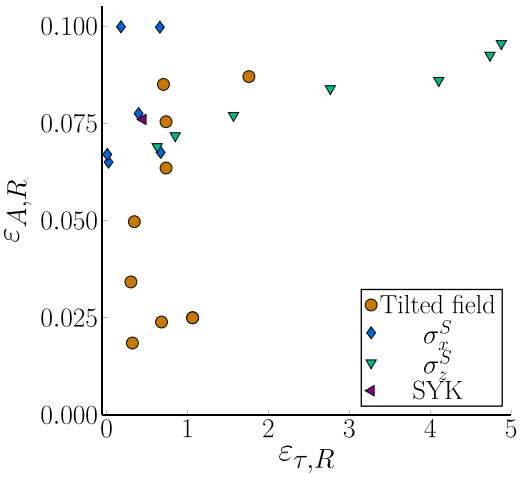

FIG. 6. Relative area error $\varepsilon_{A,R}$ (with threshold $a = 0.1$) versus relaxation time error $\varepsilon_{\tau,R}$ (with threshold $g = 0.03$) for all models considered. All R lie between 1 and 8.

Fig. 12. Both examples feature a rather large equilibration time scale. Numerically calculated exact correlation functions for two sets of parameters are shown further below in Figs. 12 and 13. The curves are obtained using a numerical approach based on quantum typicality [26].

C. Numerical equilibration times

We now study how the area estimation criterion can be used to determine the relevant R to achieve a reasonable approximation of τ. In Figs. 5 and 6 we show the relaxation-time error $\varepsilon_{\tau,R}$ versus the area error $\varepsilon_{A,R}$, for the area-error thresholds $a = 0.25$ and $a = 0.1$. In both cases, we choose $g = 0.03$ as the threshold value to define equilibration times τ, τ_a from the numerically calculated curves [26]. While there is no functional dependence visible between $\varepsilon_{A,R}$ and $\varepsilon_{\tau,R}$, one may conclude that, for all cases shown, whenever the area error is below a reasonably small threshold, this assures that $\varepsilon_{\tau,R}$ is also sufficiently small, allowing one to estimate τ from τ_a, at least within an order of magnitude. (A factor 12 for $a = 0.25$ and factor 5 for $a = 0.1$.) Note that points corresponding to, e.g., the largest R do not systematically correspond to smallest $\varepsilon_{\tau,R}$ or $\varepsilon_{A,R}$. Therefore, the area estimation appears to be a useful and easily accessible tool to determine a minimal R for a satisfactory approximation of the correlation function in terms of a finite fraction (B2).

Figures 7 and 8 show exact versus approximated relaxation times for all models considered, again for the R determined by the area threshold $a = 0.25$ and $a = 0.1$. As already visible in Figs. 5 and 6, one finds that approximated and exact relaxation times do not differ substantially from each other. Figures 7 and 8 also show that our models cover a quite large range of equilibration time scales, from fast decay for the tilted field model to slow (exponential) relaxation and oscillation for the spin coupled to a bath model [26]. In order to relate our

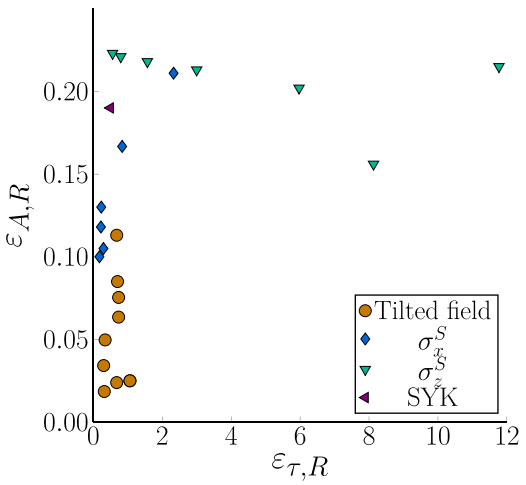

FIG. 5. Relative area error $\varepsilon_{A,R}$ (with threshold $a = 0.25$) versus relaxation time error $\varepsilon_{\tau,R}$ (with threshold $g = 0.03$) for all models considered. All R lie between 1 and 4.

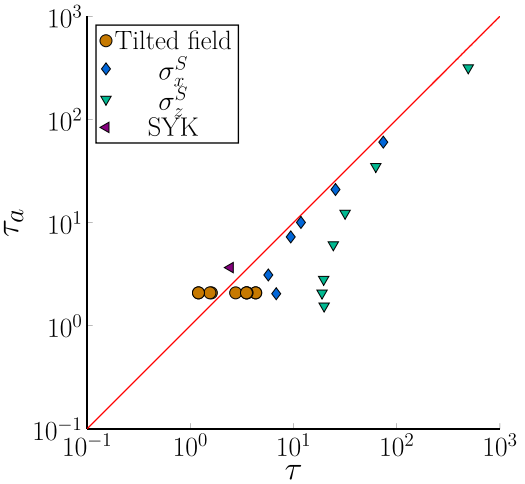

FIG. 7. Correct equilibration time τ versus approximated equilibration time τ_a, with R from area threshold $a = 0.25$ and equilibration-time threshold $g = 0.03$, for all models considered. All R lie between 1 and 4.

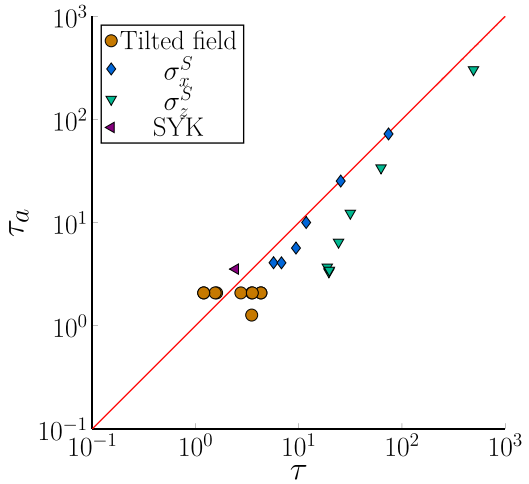

FIG. 8. Correct equilibration time τ versus approximated equilibration time τ_a, with R from area threshold $a = 0.1$ and equilibration-time threshold $g = 0.03$, for all models considered. All R lie between 1 and 8.

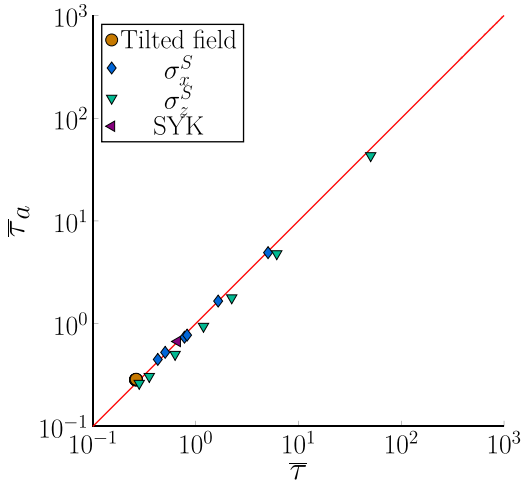

FIG. 10. Correct averaged equilibration time $\bar{\tau}$ versus approximated averaged equilibration time $\bar{\tau}_a$, with R from area threshold $a = 0.1$, for all models considered. All R lie between 1 and 8.

approach to the literature we introduce a further equilibration time defined by the time-averaged quantity

$$\bar{\tau} = \int_0^\infty |C(t)|^2\, dt, \quad \bar{\tau}_a = \int_0^\infty |C^R(t)|^2\, dt, \qquad (22)$$

for both the correct and the approximated correlation functions. This definition essentially corresponds to the equilibration time regarded in [11]. The times (22) are less sensitive against the detailed shape of the respective correlation function and upswings at later times than τ and τ_c based on thresholds. Figures 9 and 10 show exact versus approximated time-averaged relaxation times for all models considered, again for the R determined by the area threshold $a = 0.25$ and $a = 0.1$. As expected the agreement is even better than for the relaxation times based on thresholds. To further demonstrate the strength of our approach, we compare our approximation of the time-averaged equilibration time with an estimate of an upper bound of the equilibration time derived in [11], which is depicted in Fig. 11. In [11], this bound p is specified to be proportional to $1/\sqrt{\partial^2 C_0(t=0)/\partial t^2}$, which in the Lanczos or Mori formulation amounts to $\propto 1/b_1$. (For simplicity, we assume the proportionality constant to be 1.) We also note that a somewhat similar approach to describe the autocorrelation function with help of the first few coefficients b_n with the emphasis on b_1 was recently undertaken in [27].

Although there are limitations to this comparison, one may observe that our estimated time-averaged equilibration times are systematically much closer to the solid line, which represents the case when actual equilibration time and the approximate one coincide. For the spin coupled to a bath model, the approximation from [11] yields a constant for the σ_x^S component and a square root dependence in the double logarithmic plot for the σ_z^S component, for the small coupling-large equilibration time cases. Note that the slow oscillation for the σ_x^S case [26] is basically excluded in [11], because the frequency

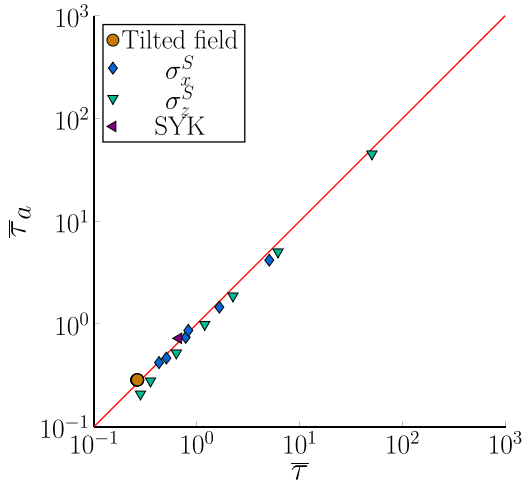

FIG. 9. Correct averaged equilibration time $\bar{\tau}$ versus approximated averaged equilibration time $\bar{\tau}_a$, with R from area threshold $a = 0.25$, for all models considered. All R lie between 1 and 4.

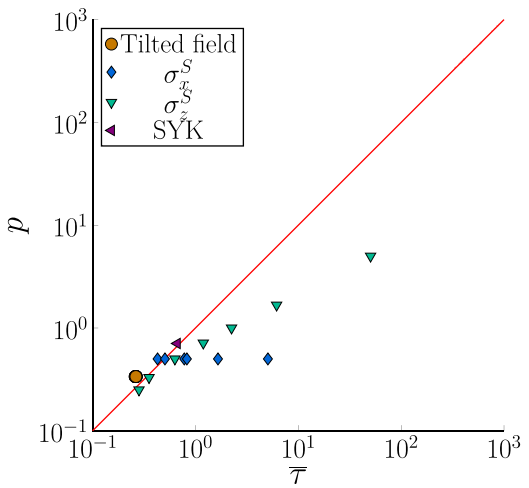

FIG. 11. Correct averaged equilibration time $\bar{\tau}$ versus bound p from [11], for all models considered.

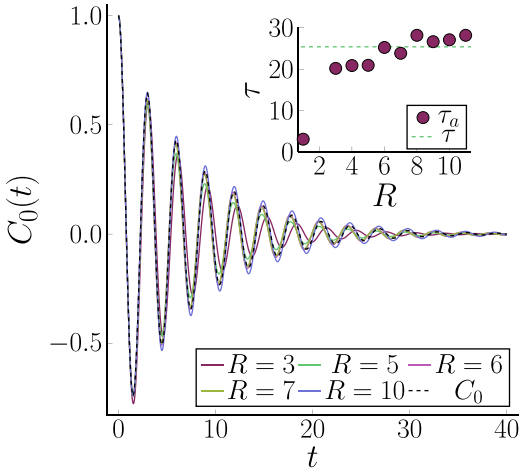

FIG. 12. Actual and approximated correlation functions for different values of R for σ_x^S, $\lambda = 0.5$ in the model of a spin-1/2 coupled to a bath. Inset shows equilibration times of approximated correlation functions for different values of R with equilibration-time threshold $g = 0.03$.

distribution is not unimodal. Additionally, the approach in [11] systematically fails for examples where the variance of the Fourier transform of the correlation function does not exist, as explained in [14], which applies for the exponential relaxation for the σ_z^S case. Along these lines the latter two examples yield substantially worse comparisons between approximated equilibration time and bound than the others.

Beyond a mere estimation of equilibration time, we propose that the "terminated" continued fraction (5) may give a reasonable approximation for the actual correlation function itself. To analyze this feature, we show in Figs. 12 and 13 approximated correlation functions for different values of R for examples that represent cases where our estimation for the equilibration time works best and worst, i.e., σ_x^S for $\lambda = 0.5$ (best) and σ_z^S for $\lambda = 1.0$ (worst) for the model of a spin-1/2 coupled to a bath. (The examples are chosen according to the smallest and largest relaxation time error $\varepsilon_{\tau,R}$ for area error threshold $a = 0.1$ and equilibration-time threshold $g = 0.03$). One finds a very good agreement even for small values of R for the good case and there is no severe qualitative difference in the behavior in the worst case. For both cases one may deduce that the disagreement becomes smaller for growing R and that there is a convergence for large R, although this behavior is not robust for small R.

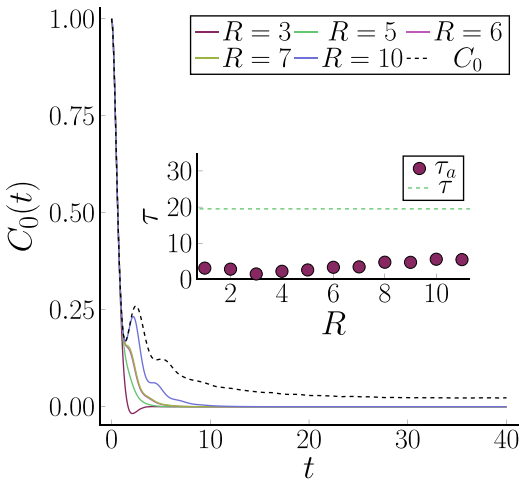

FIG. 13. Actual and approximated correlation functions for different values of R for σ_z^S, $\lambda = 1.0$ in the model of a spin-1/2 coupled to a bath. Inset shows equilibration times of approximated correlation functions for different values of R with equilibration-time threshold $g = 0.03$.

IV. CONCLUSION

We have demonstrated that descriptions of the autocorrelation dynamics in the recursive (Lanczos algorithm) and Mori formulations are equivalent and, with the help of Laplace transforms, can be recast in terms of a continued fraction expansion. Using this technique we introduced an approximation $C^R(t)$ to the autocorrelation function $C(t)$ that is fully determined by a small number of the first R Lanczos coefficients and therefore easy to evaluate numerically in most situations. We have compared suitably defined equilibration times for an actual exact correlation function and the approximation and found that the latter gives a reasonable estimation for the former. In order to control the precision of our approximation, we introduced a formalism based on an area measure, which evaluates the area under $C(t)$, as an essential part of our approach. This measure is very simple to evaluate and is considered beforehand to determine the minimal necessary number R of Lanczos coefficients to achieve the desired level of accuracy with great efficiency. We have numerically validated this approach by comparing how the quality of equilibration time estimation is correlated with the precision in estimating the area measure. We numerically considered several archetypal quantum models that exhibit a variety of different relaxation behaviors and a broad range of equilibration time scales.

We envision our approximation scheme for $C(t)$ in terms of $C^R(t)$ to be useful for various applications beyond an equilibration time estimation. Moreover, extending the approach to finite temperature correlation is an interesting topic for future research.

ACKNOWLEDGMENTS

This work has been funded by the Deutsche Forschungsgemeinschaft (DFG), under Grants No. 397107022 (GE 1657/3-2), No. 397067869 (STE 2243/3-2), and No. 397082825, within the DFG Research Unit FOR 2692, under Grant No. 355031190. A.D. is supported by the NSF under Grant No. PHY-2310426. We thank L. Knipschild and R. Heveling for fruitful discussions.

APPENDIX A: RECURSIVE METHOD AND LANCZOS COEFFICIENTS

Lanczos coefficients emerge as a part of the so-called recursion method. The object of interest is the autocorrelation function of the form

$$C(t) = \mathrm{Tr}\{O(t)O\} \tag{A1}$$

with some pertinent observable O. Here, $O(t)$ denotes the time dependence in the Heisenberg picture, $O(t) = e^{iHt}\, O\, e^{-iHt}$, induced by corresponding Hamiltonian H ($\hbar$ set to 1).

In Liouville space, i.e., the Hilbert space of observables, the elements O can be denoted as states $|O)$. The time evolution is then induced by the Liouville superoperator defined as $\mathcal{L}|O) = |[H, O])$. A suitable inner product is given by $(O_1|O_2) = \mathrm{Tr}\{O_1^\dagger O_2\}$, which in turn defines a norm $\|O\| = \sqrt{(O|O)}$. The correlation function $C(t)$ may then be written as $C(t) = (O|e^{i\mathcal{L}t}|O)$.

Now, one may iteratively construct a set of observables O_n starting with the "seed" $O_0 = O$, where O is assumed to be normalized, i.e., $(O_0|O_0) = 1$. We set $b_1 = \|\mathcal{L}O_0\|$ and $|O_1) = \mathcal{L}|O_0)/b_1$. One can now employ the (infinite) iteration scheme

$$|Q_n) = \mathcal{L}|O_{n-1}) - b_{n-1}|O_{n-2}), \tag{A2}$$

$$b_n = \|Q_n\|, \tag{A3}$$

$$|O_n) = |Q_n)/b_n, \tag{A4}$$

where $\{|O_n)\}$ constitute the Krylov basis and b_n are the Lanczos coefficients, which are real and positive and the crucial constituent in our analysis [29].

Using the Lanczos algorithm, one may cast the time evolution of the components of a vector $\vec{x}$, defined as $x_n(t) = i^{-n}(O_n|O(t))$, into the form

$$\dot{\vec{x}} = L\,\vec{x} \tag{A5}$$

with the matrix L,

$$L = \begin{pmatrix} 0 & -b_1 & 0 & 0 & \cdots \\ b_1 & 0 & -b_2 & 0 & \cdots \\ 0 & b_2 & 0 & -b_3 & \cdots \\ \vdots & \vdots & \vdots & \vdots & \ddots \end{pmatrix}, \tag{A6}$$

which is similar to the standard Schrödinger equation. Then, the first component of $\vec{x}$ is the correlation function of interest, $x_0(t) = C(t)$. The initial condition is always given by $x_n(0) = \delta_{0n}$.

Note that L is here an anti-Hermitian tridiagonal matrix, but the components x_n are all real numbers which is very convenient for the following analysis.

For clarity, the above set of equations may also be written as

$$\dot{x}_0(t) = -b_1 x_1(t), \tag{A7}$$

$$\dot{x}_n(t) = b_n x_{n-1}(t) - b_{n+1} x_{n+1}(t), \quad n \geqslant 1. \tag{A8}$$

That is, the dynamics of the correlation function $C(t)$ may be calculated as occupation amplitude of the "first" site in a one-dimensional noninteracting hopping model without specifying any details of H and A.

In the following, we assume that the final Lanczos coefficient b_{m+1} is equal to 0 (for possibly large m). This is always the case for systems with a finite-dimensional Hilbert space. Doing so closes the infinite set of equations in the Lanczos formulation (A5), which in turn allows us to perform the Laplace transform of the now finite set of equations to arrive at the following finite "continued" fraction expansion. Say, when $m = 3$ and $b_4 = 0$ we have explicitly

$$\tilde{x}_0(s) = \cfrac{1}{s + \cfrac{b_1^2}{s + \cfrac{b_2^2}{s + \cfrac{b_3^2}{s}}}}. \tag{A9}$$

Here, $\tilde{x}_0(s)$ is the Laplace transform of $x_0(t)$.

The continued fraction representations of the equations of motion (A8) were given in [17].

In practice the complexity of evaluating b_n numerically quickly grows with n, such that only a handful of first b_n are usually available. For a local operator O and a Hamiltonian with local interactions the first coefficients b_n, up to n of the order of the system size, are system size independent.

APPENDIX B: MORI FORMULATION OF DYNAMICS

In the previous section we presented the description of the correlation function in terms of the recursive method and the Lanczos algorithm. There is an alternative approach of Mori [30,31], with the time evolution specified by a set of functions $C_n(t)$ satisfying a coupled series of Volterra equations,

$$\dot{C}_n(t) = -\Delta_{n+1}^2 \int_0^t C_{n+1}(t - t')C_n(t')dt', \tag{B1}$$

where $C_0(t) = x_0(t) = C(t)$ is the correlation function itself. Each function satisfies $C_n(0) = 1$ and $\Delta_{n+1}^2 C_{n+1}(t)$ acts as a memory kernel for the dynamics of $C_n(t)$. The value of constants Δ_{n+1}^2 defines the value of the memory kernels at time $t = 0$.

Both dynamical descriptions are equivalent [32] and as we show momentarily the constants Δ_n are equal to the Lanczos coefficients b_n.

Within the Mori formulation (B1) the condition $b_{m+1} = 0$ is equivalent to the condition that the normalized memory kernel $C_m(t)$ is a right-continuous Heaviside step function $\Theta(t)$, i.e., $C_m(t)$ decays arbitrarily slowly or rather not at all. In this case, Laplace transforming (B1) [assuming $m = 3$ and $C_3(t) = \Theta(t)$] yields

$$\tilde{C}_0(s) = \cfrac{1}{s + \cfrac{\Delta_1^2}{s + \cfrac{\Delta_2^2}{s + \cfrac{\Delta_3^2}{s}}}}, \tag{B2}$$

where $\tilde{C}_0(s) = \tilde{x}_0(s)$ is again the Laplace transform of the autocorrelation function. Continued fraction representations in the context of the Mori approach have been formulated in [33].

Comparing the Laplace transforms (A9) and (B2) readily yields that both dynamical descriptions are equivalent and that $\Delta_n = b_n$.

The recursive and Mori methods can both be understood from the lens of completely integrable dynamics; see [34].

As a spin-off observation, not related to the following analysis, we note that the time evolution of $C_n(t)$ ($n \geqslant 1$) corresponds to the time evolution of $x_n(t)$ but with a time evolution operator obtained by deleting the first n rows and columns of L. [Also, the initial conditions are different: $C_n(0) = 1$ and $x_n(0) = 0$ for $n \geqslant 1$].

[1] C. Gogolin and J. Eisert, Equilibration, thermalisation, and the emergence of statistical mechanics in closed quantum systems, Rep. Prog. Phys. **79**, 056001 (2016).

[2] P. Reimann, Foundation of statistical mechanics under experimentally realistic conditions, Phys. Rev. Lett. **101**, 190403 (2008).

[3] L. Knipschild and J. Gemmer, Modern concepts of quantum equilibration do not rule out strange relaxation dynamics, Phys. Rev. E **101**, 062205 (2020).

[4] S. Goldstein, T. Hara, and H. Tasaki, Time scales in the approach to equilibrium of macroscopic quantum systems, Phys. Rev. Lett. **111**, 140401 (2013).

[5] A. S. L. Malabarba, L. P. García-Pintos, N. Linden, T. C. Farrelly, and A. J. Short, Quantum systems equilibrate rapidly for most observables, Phys. Rev. E **90**, 012121 (2014).

[6] P. Reimann, Typical fast thermalization processes in closed many-body systems, Nat. Commun. **7**, 10821 (2016).

[7] Vinayak and M. Žnidarič, Subsystem dynamics under random hamiltonian evolution, J. Phys. A: Math. Theor. **45**, 125204 (2012).

[8] F. G. S. L. Brandão, P. Ćwikliński, M. Horodecki, P. Horodecki, J. K. Korbicz, and M. Mozrzymas, Convergence to equilibrium under a random Hamiltonian, Phys. Rev. E **86**, 031101 (2012).

[9] L. Masanes, A. J. Roncaglia, and A. Acín, Complexity of energy eigenstates as a mechanism for equilibration, Phys. Rev. E **87**, 032137 (2013).

[10] S. Goldstein, T. Hara, and H. Tasaki, Extremely quick thermalization in a macroscopic quantum system for a typical nonequilibrium subspace, New J. Phys. **17**, 045002 (2015).

[11] A. M. Alhambra, J. Riddell, and L. P. García-Pintos, Time evolution of correlation functions in quantum many-body systems, Phys. Rev. Lett. **124**, 110605 (2020).

[12] L. P. García-Pintos, N. Linden, A. S. L. Malabarba, A. J. Short, and A. Winter, Equilibration time scales of physically relevant observables, Phys. Rev. X **7**, 031027 (2017).

[13] R. Hamazaki, Speed limits for macroscopic transitions, PRX Quantum **3**, 020319 (2022).

[14] R. Heveling, L. Knipschild, and J. Gemmer, Comment on "Equilibration time scales of physically relevant observables", Phys. Rev. X **10**, 028001 (2020).

[15] J. Richter, J. Gemmer, and R. Steinigeweg, Impact of eigenstate thermalization on the route to equilibrium, Phys. Rev. E **99**, 050104(R) (2019).

[16] J. Richter, M. H. Lamann, C. Bartsch, R. Steinigeweg, and J. Gemmer, Relaxation of dynamically prepared out-of-equilibrium initial states within and beyond linear response theory, Phys. Rev. E **100**, 032124 (2019).

[17] R. Haydock, The recursive solution of the Schrödinger equation, Comput. Phys. Commun. **20**, 11 (1980).

[18] D. E. Parker, X. Cao, A. Avdoshkin, T. Scaffidi, and E. Altman, A universal operator growth hypothesis, Phys. Rev. X **9**, 041017 (2019).

[19] V. S. Viswanath and G. Müller, *The Recursion Method: Application to Many-body Dynamics* (Springer, New York, 2008).

[20] V. S. Viswanath and G. Müller, Recursion method in quantum spin dynamics: The art of terminating a continued fraction, J. Appl. Phys. **67**, 5486 (1990).

[21] J. Maldacena and D. Stanford, Remarks on the Sachdev-Ye-Kitaev model, Phys. Rev. D **94**, 106002 (2016).

[22] A. Dymarsky and M. Smolkin, Krylov complexity in conformal field theory, Phys. Rev. D **104**, L081702 (2021).

[23] A. Avdoshkin, A. Dymarsky, and M. Smolkin, Krylov complexity in quantum field theory, and beyond, J. High Energy Phys. 06 (2024) 066.

[24] J. Wang, M. H. Lamann, J. Richter, R. Steinigeweg, A. Dymarsky, and J. Gemmer, Eigenstate thermalization hypothesis and its deviations from random-matrix theory beyond the thermalization time, Phys. Rev. Lett. **128**, 180601 (2022).

[25] R. Heveling, J. Wang, and J. Gemmer, Numerically probing the universal operator growth hypothesis, Phys. Rev. E **106**, 014152 (2022).

[26] The numerical calculation of the correct autocorrelation function is done by the use of dynamical quantum typicality; see, e.g., Ref. [28].

[27] R. Zhang and H. Zhai, Universal hypothesis of autocorrelation function from krylov complexity, Quantum Front **3**, 7 (2023).

[28] T. Heitmann, J. Richter, D. Schubert, and R. Steinigeweg, Selected applications of typicality to real-time dynamics of quantum many-body systems, Z. Naturforsch. A **75**, 421 (2020).

[29] F. Cyrot-Lackmann, On the electronic structure of liquid transitional metals, Adv. Phys. **16**, 393 (1967).

[30] H. Mori, Transport, collective motion, and Brownian motion, Prog. Theor. Phys. **33**, 423 (1965).

[31] C. Joslin and C. Gray, Calculation of transport coefficients using a modified Mori formalism, Mol. Phys. **58**, 789 (1986).

[32] G. Moro and J. H. Freed, Classical time-correlation functions and the Lanczos algorithm, J. Chem. Phys. **75**, 3157 (1981).

[33] H. Mori, A continued-fraction representation of the time-correlation functions, Prog. Theor. Phys. **34**, 399 (1965).

[34] A. Dymarsky and A. Gorsky, Quantum chaos as delocalization in krylov space, Phys. Rev. B **102**, 085137 (2020).